Electrochemical Performance of Coal-Based Needle Coke Anode for Lithium Ion Batteries

Yuan Gao[1, a *], Jing Xia[1], Cuifeng Mu[2], Dakui Zhang [2], Shuxiang Li[1] and Zhanqiang Xue[2]

[1]Ansteel Beijing Research Institute CO., LTD., Beijing, China

[2]Angang Chemical Technology CO., LTD., Anshan 114000, China

[a]email: gaoyuan0121@163com

Abstract. Lithium-ion capacitors (LICs) with the capability of high energy and high power are considered to be attractive for advanced energy storage applications. However, the design and fabrication of suitable electrode materials with desirab-le properties by a facile approach using cost-effective precursors are still a great challenge. In this work, we have utilized needle cokes, an commercial carbon material with high carbon content and soft carbon structure, as a single carbon source for anode material. A lithium-ion battery fabricated using four kinds of needle cokes exhibits a maximum high energy density of 1357mAhg-1. Systematic characterization analysis demonstrates that unique characteristics of the green coke including large interlayer spacing, turbostratic and disordered microstructures that are composed of surface defects, nanopores or voids, and graphitic domains. That contribute synergistically to the outstanding performance of the needle coke-based LIC. More importantly, anode materials from a single source is an effective way for high value-added utilization of needle coke at the commercial level.

Keywords: Needle Coke, Lithium Ion Batteries, Coal-Based Coke, Anode Materials.

1. Introduction

Lithium-ion batteries have stimulated extensive research studies due to their high-energy storage, which enables the fabrication of smaller and lighter batteries for mobile electronics . Various types of carbonaceous material such as graphite1, 2, carbon fibers3, thermal decomposition products of polymers, pyrolytic carbon , petroleum coke and coal tar pitch coke have been proposed for the anode materials of lithium-ion battery4, 5.

As a kind of soft carbon, needle coke has the advantages of low cost , good graphite microcrystalline structure and good electrical conductivity6. At present, there are still some shortcomings in the needle coke used for lithium-ion battery anode materials7. The surface of needle coke is easy to react irreversibly with electrolyte, resulting in the reduction of coulombic efficiency. solvent co-embedding caused the appearance of the reversible capacity for the battery, material volume expansion and poor cycling performance, etc8.

In this work, we report to use coal-based green needle coke, calcined cokes and their powdery by-products as the anode material to investigate the electrochemical performance for lithium ion batteries.The purpose of this paper is intended to analysis the reasons of current problems, and seeks for solutions in the development of more reliable and safer lithium rechargeable batteries.

2. Experimental

2.1 Materilas

The coal-based green and calcined needle cokes fabricated at 500 ºC and 1400ºC respectively, were purchased from Ansteel Group CO., LTD..Coke. Powder was coke with particle diameter less than 1mm produced in the coking and calcination process . Theirs volatile, ash content, density and sulfur residue value were shown in table 1.

Table 1. The properties of the coal-based needle coke

	Density (g/cm^3)	S(%)	Ash (%)	Volatile (%)	Moisture (%)	Tap density (g/cm^3)	Resistivity
Green coke	1.401	0.45	0.39	6.60	5.3	-	-
Green coke powder	1.427	0.44	0.13	5.58	2.36	-	-
Calcined coke	2.14	0.41	0.29	0.45	0.05	0.93	471
Calcined coke power	2.13	0.41	0.16	0.32	0.07	0.94	439

2.2 Characterization

The microstructure of the sample was observed by the field emission scanning electron microscope (FESEM, Gemini 560), and the X-ray diffraction (XRD, Bruker D8 Advance) spectroscope with a Cu Kα radiation source (1.5405 Å), tube voltage 40 kV, tube current 30 mA, scanning range 10-90° and scanning rate 10° min^{-1} was employed to analyze the crystalline structures of samples[9-11]. The Raman spectra were recorded by a Renishaw (inVia DM2700M micro-Raman) spectrometer[12]. All the electrochemical tests were conducted using coin cells (CR2025). The working electrodes were prepared by spreading the mixed slurry of active material, Super P and sodium alginate in water with a weight ratio of 7:2:1 onto copper foil. Then they were dried at 120 °C in vacuum for 12 h. The electrolyte was a solution of 1 M $LiPF_6$ in ethylene (EC) and dimethyl carbonate (DMC) (v:v=1:1). A lithium foil was used as the counter electrode. All the operations were performed in a glove box under argon atmosphere. The discharge/charge tests were carried out on a Land BT2000 battery test system at room temperature. The voltage ranged from 0.01 to 2 V with a current density of 100 mA/g[13, 14].

3. Results and Discussion

Figure 1 shows the morphology of four kinds of needle coke materials. It can be seen from the figure that all four kinds of needle coke are flake particles, among which there are still many irregular particles on the raw coke surface and raw coke block, mainly because the coking temperature is only about 500℃, and more amorphous carbon structures are still retained. The structure of cooked coke surface and cooked coke block is similar to the appearance of natural graphite. Due to the high temperature treatment of 1400℃, the crystal surface has increased.

Thermogravimetric analysis was carried out for the four materials respectively. It can be seen from Figure 2 that the four materials were almost completely burned under air atmosphere at 10°C/min. Earlier weight loss in green coke powder combustion compared to green coke was due to more lattice defects and active sites of the powder, and the same phenomenon can be observed in the combustion process of calcined coke and its powder.The green coke material begins to react with air at around 480℃, the material begins to lose weight, and the reaction is completed at 800℃, while the reaction temperature range of the calcined coke is between 521 and 928℃. The maximum weight loss (DTGmax) occurred corresponding to combustion of green coke powder at 1230μg/min, which is contributed to the disorder sturcture and active site in the edge[15-17]. A shift in calcined coke and its powder DTGmax to higher temperatures was also observed compared to that in green coke combustion.

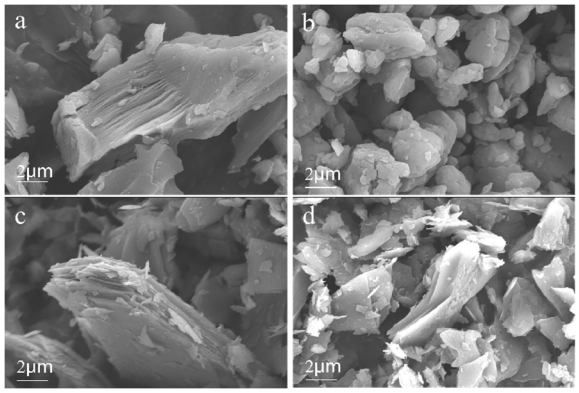

Figure 1. Typical SEM images of needle cokes (a.Green coke; b.Green coke powder; c.Calcined coke; d.Calcined coke powder)

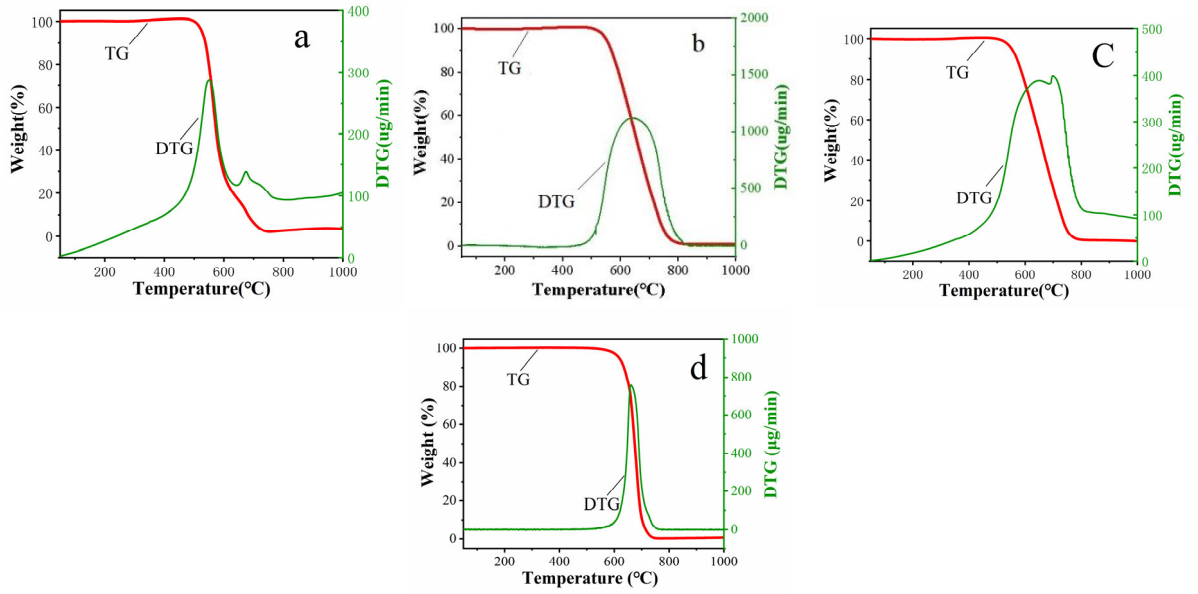

Figure 2. TG and DTG curves of needle cokes at a heating rate of 10 ºC/min in an air atmosphere (a.Green coke; b.Green coke powder; c.Calcined coke; d.Calcined coke powder)

Figure 3 shows the Raman spectra of cokes. The D peak near 1440cm^{-1} is caused by the symmetric stretching vibration of SP^2 carbon atoms in the aromatic ring, corresponding to defects and amorphous structures in coke[18], while the G peak near 1530cm^{-1} is caused by the stretching vibration between SP^2 carbon atoms corresponding to a regular graphite structure. The peak intensity comparion of peak G and peak D (i.e. S_G/S_D) is usually used to measure the degree of regular structure of coke

According to the calculation of strength of peak G and peak D , the S_G/S_D values of green coke, green coke powder, calcined coke and calcined coke powder are 0.48,0.44, 0.70, 0.67, respectively(Table 2). The S_G/S_D value of calcined coke was significantly higher than that of green coke, indicating that the defects of raw coke were reduced and the structure was more regular after high temperature treatment at 1400 ºC.

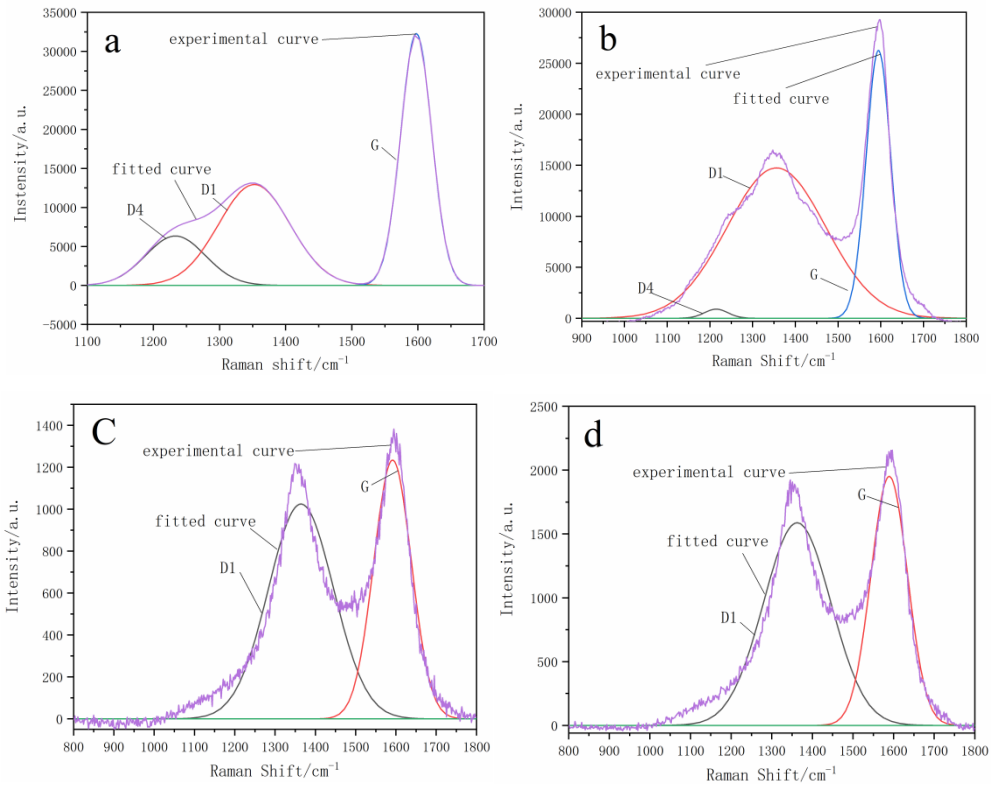

Figure 3. Raman spectra of cokes (a.Green coke; b.Green coke powder; c.Calcined coke; d.Calcined coke powder)

Table.2. the S_G/S_D values of cokes

Samples	green coke	green coke powder	calcined coke	calcined coke powder
S_G/S_D	0.48	0.44	0.70	0.67

As shown in Figure 4, The X-ray powder diffraction patterns of all the coke samples are typical of structured carbon materials with distinct reflection reflexes (002) and (004) from the (00*l*) family and two-dimensional[19, 20]. The diffraction peak of green coke powder, green coke, calcined coke powder and calcined coke(002) is 26.06º, 26.06º,26.15º, 26.15º, respectively. No reflex from the (101) plane is seen for any sample. That indicates poor orientation of the graphene layers.However, compared with the diffraction profiles of the green cokes ,the profiles of the calcined cokes reflexes (002) is sharper, indicating that the calcined cokes has a more regular graphite crystal structure and the powders has more disorder structures, which is consistent with the results of the Raman test above.

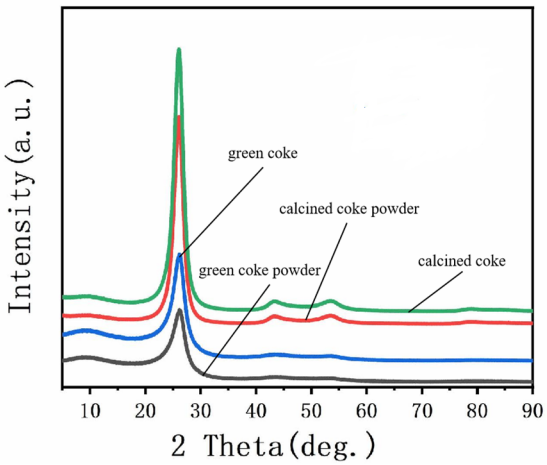

Figure 4. X-ray powder diffraction pattern of coke samples

Fig. 5a shows the initial discharge-charge curves of all the samples at the current density of 100 mAg^{-1} between 0.005 and2.0V. The initial discharge capacity is 820 $mAhg^{-1}$ for the green coke,1357$mAhg^{-1}$ for the green coke power, 434 $mAhg^{-1}$ for the calcined coke and 467 $mAhg^{-1}$ for the calcined coke powder, while their initial charge capacities are 368, 464, 277 and 268 $mAhg^{-1}$,respectively Thus, the initial coulomb efficiency of the samples is in the order of the calcined coke (63.8%) > the calcined coke powder (57.4%) > the green coke(45.0%) > the green coke powder (34.2%). The much lower initial coulombic efficiency of non-calcined coke (the green coke and its powder) than those of the calcined coke (the calcined coke and its powder) may be because there are many defects on the surface and internal porosities in the non-calcined coke, which raise more secondary reactions involving electrolyte decomposition between electrode and electrolyte resulting in a high irreversibility (low columbic efficiency)[21].As a result, more SEI flms will be generated as more lithium ions will participate in an irreversible reaction.

The cycling performance in Fig.6 shows that the charge capacities of green coke; green coke powder; calcined coke; calcined coke powder are around 368, 464, 268 and 277 $mAhg^{-1}$ at the first cycle, and 350, 328, 268, and 284 $mAhg^{-1}$ after 300 cycles.

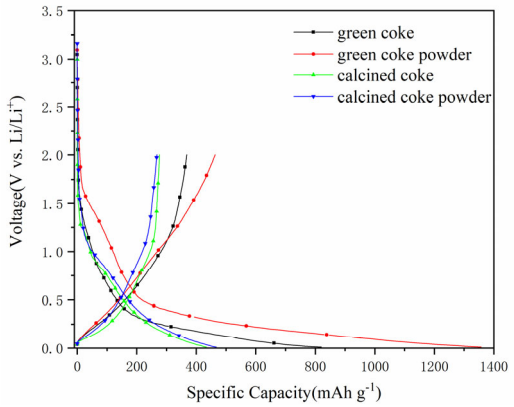

Figure 5. The charge−discharge performance of the lithium-ion battery constructed using cokes as anode materials

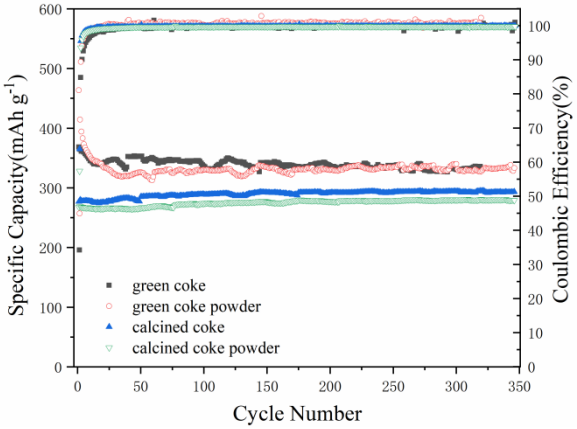

Figure 6. Cycling performance of the cokes as anode materials at 100 mAg^{-1}

The rate performances of all the samples at different current densities between 0.005 and 2.0V are shown in Fig. 7. At low current densities (50 and 100 mAg^{-1}), the observed results are consistent with that obtained in the above cycling test. However, the distinct difference in electrochemical properties is observed for these samples when the current density is increased to 500 and 1000 mAg^{-1}. The average charge capacities of green coke; green coke powder; calcined coke; calcined coke powder are 184, 200, 180 and 196 $mAhg^{-1}$ at 500 mAg^{-1}, and 138, 149, 157, and 178 $mAhg^{-1}$ at 1000 mAg^{-1}, respectively.Calcined coke and its powder have much higher capacity than that of green coke and its powder at the current density of 1000mAg^{-1}, because the porous structure of calcined coke could provide shorter and faster transport pathways for both electrons and Li ions.

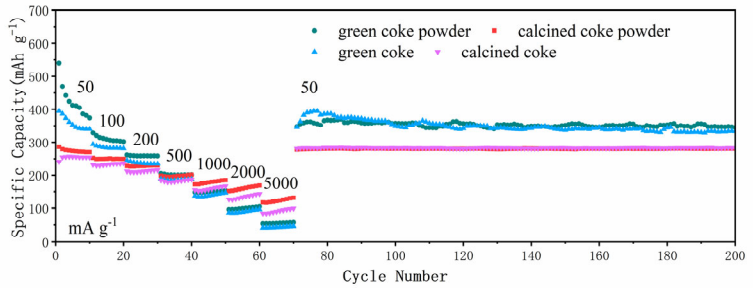

Figure 7. Rate performance at different current densities of the cokes as anode materials

Cyclic voltammograms in Fig.8 reveal that a distinct cathodic peak attributed to the decomposition of electrolyte and the formation of SEI film at 0.2 V can be observed during the first sweep for calcined coke and its powder, which is attributed to the better orientation of the graphene layers. Only a very small cathodic peak is observed for green coke and its powder, which indicates that amorphous carbon on the surface of an electrode decrease the contact areas between coke and electrolyte and can effectively suppress solvent decomposition on the carbon electrode. The peaks observed at around 0.1 and 0.01 V are assignable to the lithiation process of graphite. It can be seen that the oxidation peaks of green cokes are shifted toward lower potentials, compared to calcined cokes, indicating that green cokes easily undergo the electrochemical oxidation by accepting electrons during first lithium deintercalation. This is because the porous structure, and the hard carbon conductive network in green cokes could provide shorter and faster transport pathways for both electrons and Li ions.

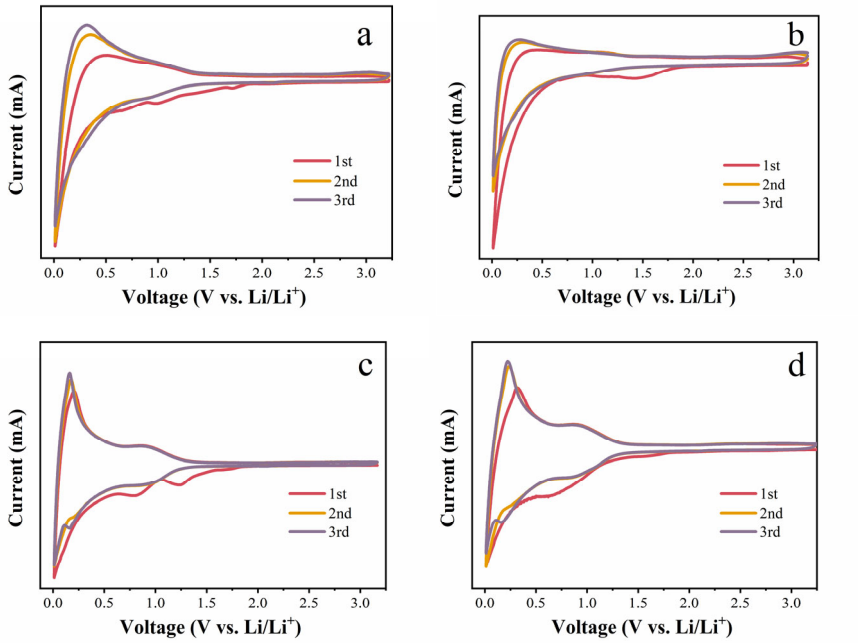

Figure 8. Cyclic voltammograms during the initial discharge-charge of the cokes as anode materials (a.Green coke; b.Green coke powder; c.Calcined coke; d.Calcined coke powder)

Fig. 9 shows the electrochemical impedance spectrum before cycling of all the cokes. The impedance plot is consisted of one semicircle curve that corresponds to the resistance of the Li ion transfer through SEI layers in the high frequency range, and a straight line to the charge transfer resistance at the electrode–electrolyte interface and the Li ion Warburg diffusion resistance in the solid electrode material in the low frequency range. Although the slopes of their straight lines are very similar, the size of their semicircles is different, going as green coke＞green coke powder＞calcined coke＞calcined coke powder. It should be pointed out that the calcined coke powder show much smaller semicircle than those of green cokes, indicating a lower electrochemical reaction resistance in the green cokes electrode, probably because of the presence of the porous structure, and the disordered conductive network in green cokes. It can be seen that the electrochemical reaction

resistances of calcined cokes are lower than those of green cokes, respectively. It is considered that the electronic conductivity of carbon could be improved after calcination(1400°C). The calcined coke powder has the lowest resistance, thus its rate property is the best of all the cokes. It is concluded that pore structure and the disordered conductive network can improve the rate performance.

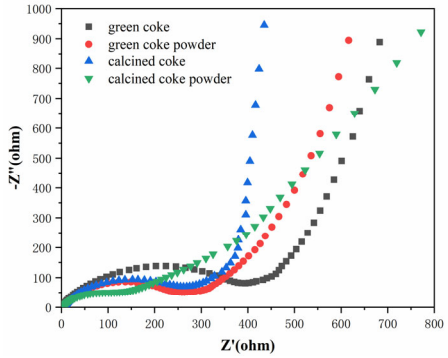

Figure 9. Electrochemical impedance spectrum of the cokes as anode materials

4. Summary

we have utilized four kinds of needle cokes as a single carbon source for anode material. The SEM image, Thermogravimetric analysis Raman spectra and X-ray powder diffraction pattern show that unique characteristics of the green coke including large interlayer spacing, turbostratic and disordered microstructures that are composed of surface defects, nanopores or voids, and graphitic domains are retained, which deliver the outstanding performance of the needle coke-based LIC of 1357mAhg^{-1}. However, calcined coke and its powder have much higher capacity than that of green coke at the current density of 1000mAg^{-1}. Only a very small cathodic peak of cyclic voltammograms during the initial discharge-charge is observed for green coke and its powder, which indicates that amorphous carbon on the surface of an electrode decrease the contact areas between coke and electrolyte and can effectively suppress solvent decomposition on the carbon electrode.The size of their semicircles of the electrochemical impedance spectrum is different, going as green coke＞green coke powder＞calcined coke＞calcined coke powder.

References

[1] Ma, Z.-F.; Yuan, X.-Z.; Li, D.; Liao, X.-Z.; Hu, H.-P.; Ma, J.-Q.; Wang, J.-F., Structural and electrochemical characterization of carbonaceous mesophase spherule anode material for rechargeable lithium batteries. Electrochemistry Communications 2002, 4 (2), 188-192.

[2] Wang, Y.-G.; Egashira, M.; Ishida, S.; Korai, Y.; Mochida, I., Microstructure of mesocarbon microbeads prepared from synthetic isotropic naphthalene pitch in the presence of carbon black. Carbon 1999, 37 (2), 307-314.

[3] Imanishi, N.; Kashiwagi, H.; Ichikawa, T.; Takeda, Y.; Yamamoto, O.; Inagaki, M., Charge - Discharge Characteristics of Mesophase - Pitch - Based Carbon Fibers for Lithium Cells. Journal of The Electrochemical Society 1993, 140 (2), 315-320.

[4] Azuma, H.; Imoto, H.; Yamada, S. i.; Sekai, K., Advanced carbon anode materials for lithium ion cells. Journal of Power Sources 1999, 81 – 82, 1-7.

[5] Cao, F.; Barsukov, I. V.; Bang, H. J.; Zaleski, P.; Prakash, J., Evaluation of Graphite Materials as Anodes for Lithium-Ion Batteries. Journal of The Electrochemical Society 2000, 147 (10), 3579.

[6] Brooks, J. D.; Taylor, G. H., The formation of graphitizing carbons from the liquid phase. Carbon 1965, 3 (2), 185-193.

[7] Kang, H.-G.; Park, J.-K.; Han, B.-S.; Lee, H., Electrochemical characteristics of needle coke refined by molten caustic leaching as an anode material for a lithium-ion battery. Journal of Power Sources 2006, 153 (1), 170-173.

[8] Li, H.; Li, W., Improving cycle life and rate capability of artificial graphite anode for lithium-ion batteries by agglomeration. Materials Letters 2022, 318, 132227.

[9] Popova, A. N., Crystallographic analysis of graphite by X-Ray diffraction. Coke and Chemistry 2017, 60 (9), 361-365.

[10] Ismagilov, Z. R.; Sozinov, S. A.; Popova, A. N.; Zaporin, V. P., Structural Analysis of Needle Coke. Coke and Chemistry 2019, 62 (4), 135-142.

[11] Iwashita, N.; Park, C. R.; Fujimoto, H.; Shiraishi, M.; Inagaki, M., Specification for a standard procedure of X-ray diffraction measurements on carbon materials. Carbon 2004, 42 (4), 701-714.

[12] Chen, K.; Zhang, H.; Ibrahim, U.-K.; Xue, W.; Liu, H.; Guo, A., The quantitative assessment of coke morphology based on the Raman spectroscopic characterization of serial petroleum cokes. Fuel 2019, 246, 60-68.

[13] Wang, C.; Zhao, H.; Wang, J.; Wang, J.; Lv, P., Electrochemical performance of modified artificial graphite as anode material for lithium ion batteries. Ionics 2013, 19 (2), 221-226.

[14] Veluri, P. S.; Katchala, N.; Anandan, S.; Pramanik, M.; NarayanSrinivasan, K.; Ravi, B.; N. Rao, T., Petroleum Coke as an Efficient Single Carbon Source for High-Energy and High-Power Lithium-Ion Capacitors. Energy & Fuels 2021, 35, 9010-9016.

[15] Jiang, W.; Tran, T.; Song, X.; Kinoshita, K., Thermal and electrochemical studies of carbons for Li-ion batteries: 1. Thermal analysis of petroleum and pitch cokes. Journal of Power Sources 2000, 85 (2), 261-268.

[16] Kondrasheva, N. K.; Rudko, V. A.; Ancheyta, J., Thermogravimetric Determination of the Kinetics of Petroleum Needle Coke Formation by Decantoil Thermolysis. ACS Omega 2020, 5 (45), 29570-29576.

[17] Zhang, Z.; Huang, X.; Zhang, L.; Guo, S.; Du, H.; Chen, Z.; Wu, B.; Li, G.; Liu, D., Study on the evolution of oxygenated structures in low-temperature coal tar during the preparation of needle coke by co-carbonization. Fuel 2022, 307, 121811.

[18] Tran, T.; Yebka, B.; Song, X.; Nazri, G.; Kinoshita, K.; Curtis, D., Thermal and electrochemical studies of carbons for Li-ion batteries: 2. Correlation of active sites and irreversible capacity loss. Journal of Power Sources 2000, 85 (2), 269-278.

[19] Ren, W.; Zhang, Z.; Wang, Y.; Kan, G.; Tan, Q.; Zhong, Z.; Su, F., Preparation of porous carbon microspheres anode materials from fine needle coke powders for lithium-ion batteries. RSC Advances 2015, 5 (15), 11115-11123.

[20] Moradi, B.; Botte, G. G., Recycling of graphite anodes for the next generation of lithium ion batteries. Journal of Applied Electrochemistry 2016, 46 (2), 123-148.

[21] Wang, L.; Li, Z.; Du, C.; Han, Y.; Yang, J., High-temperature graphitization of coke and lithium storage properties of coke-based graphite. International Journal of Coal Preparation and Utilization 2023, 1-18.